

Dynamic Gadolinium-Enhanced Perfusion MRI of Prostate Cancer: Assessment of Response to Hypofractionated Robotic Stereotactic Body Radiation Therapy

Russell N. Low¹
Donald B. Fuller²
Naira Muradyan³

OBJECTIVE. The purpose of this study was to evaluate the utility of dynamic gadolinium-enhanced perfusion MRI for monitoring the response to robotic stereotactic body radiation therapy for prostate cancer.

MATERIALS AND METHODS. Eighty-seven patients with prostate cancer underwent dynamic gadolinium-enhanced MRI before robotic stereotactic body radiation therapy, and prostate volume was calculated. Pharmacokinetic analysis postprocessing software was used to generate colorized parametric maps showing perfusion of enhancing tumors. The transfer constant K^{trans} was calculated for identified tumors. Follow-up MRI was performed 2 months after treatment for 22 patients, 6 months for 71 patients, 12 months for 54 patients, and 24 months for 27 patients with repeated measurements of prostate volume and K^{trans} .

RESULTS. Perfusion MRI depicted focal enhancing prostate tumors that correlated with the biopsy results in 82 of 87 patients (94%). The median K^{trans} of tumors before robotic stereotactic body radiation therapy was 1.79 minutes⁻¹. Follow-up MRI showed decreases in the size and degree of enhancement of tumors. The median tumor K^{trans} decreased to 1.21 minutes⁻¹ 2 months, 0.39 minutes⁻¹ 6 months, 0.30 minutes⁻¹ 12 months, and 0.22 minutes⁻¹ 24 months after treatment. Prostate volume had decreased 23% 2 months, 26% 6 months, 33% 12 months, and 37% 24 months after robotic stereotactic body radiation therapy. The corresponding median prostate-specific antigen concentration before treatment was 6.45 ng/mL. After treatment, the concentration was 2.90 ng/mL at 2 months, 1.30 ng/mL at 6 months, 1.10 ng/mL at 12 months, and 0.59 ng/mL at 24 months.

CONCLUSION. Dynamic gadolinium-enhanced MRI is a useful tool for monitoring the response of prostate cancer to robotic stereotactic body radiation therapy, yielding both qualitative and quantitative data.

Keywords: dynamic contrast-enhanced MRI, functional MRI, metabolic imaging, prostate, prostate cancer

DOI:10.2214/AJR.10.6356

Received December 13, 2010; accepted after revision March 14, 2011.

¹Department of Radiology, Sharp Memorial Hospital, Sharp and Children's MRI Center, 7901 Frost St, San Diego, CA 92123. Address correspondence to R. N. Low (rlow52@yahoo.com).

²CyberKnife Centers of San Diego, San Diego, CA.

³iCAD, Inc., Nashua, NH.

AJR2011; 197:907–915

0361–803X/11/1974–907

© American Roentgen Ray Society

Monitoring the response of prostate cancer to radiation therapy is challenging [1, 2]. Prostate-specific antigen (PSA) is a protein produced by the prostate, and the concentration is elevated in patients with prostate cancer. After treatment, the radiation oncologist follows serial PSA values to monitor treatment response. Serial PSA measurements present limitations due to false-positive and false-negative results [3–7]. Prostate biopsy after radiation therapy also is prone to problems that can lead to false-positive, false-negative, and indeterminate biopsy results [2]. Because of the flaws and shortcomings of PSA measurements and biopsy after radiation therapy, improved monitoring techniques are needed.

In robotic stereotactic body radiation therapy, external radiation is delivered with a com-

pact lightweight linear accelerator mounted on a robotic arm [8]. Submillimeter accuracy for delivery of the radiation dose allows delivery of higher biologic doses to the tumor with relatively improved sparing of adjacent normal tissues. Compared with conventional external beam radiation therapy, which takes approximately 2 months to complete, stereotactic body radiation therapy takes 1 week. Application of robotic stereotactic body radiation therapy to the management of prostate cancer is being evaluated and appears promising after 5 years of follow-up [9–11].

The excellent soft-tissue contrast of MRI makes it an ideal examination for detection of prostate cancer and for monitoring of response to therapy [12–16]. Dynamic contrast-enhanced MRI (DCE-MRI) is performed after administration of extracellular gadolinium chelate contrast agents in the

TABLE 1: Clinical Data

Patient Group	n	Prostate-Specific Antigen Concentration (ng/mL)	Gleason Score					Tumor Category				
			5	6	7	8	9	T1c	T2a	T2b	T2c	T3a
Robotic stereotactic body radiotherapy alone	73	6.4	1	40	32	0	0	46	21	6	0	0
Robotic stereotactic body radiotherapy plus intensity-modulated radiotherapy	14	8.1	0	0	5	4	5	4	2	4	1	1

evaluation of differential enhancement of tumors compared with normal tissue. DCE-MRI yields information about key physiologic parameters of normal tissues and tumors [17–20]. Because tumors have increased vascular permeability owing to tumor angiogenesis, DCE-MRI can be used to detect and characterize various tumors and to monitor response to therapy [21]. After therapy, prostate cancer may have a decrease in tumor vascular permeability that can be assessed and monitored with DCE-MRI [21–24]. We performed this study to evaluate the value of perfusion DCE-MRI in monitoring the response of prostate cancer to robotic stereotactic body radiation therapy.

Materials and Methods

Between July 2006 and January 2010, 99 patients with known prostate cancer were treated with robotic stereotactic body radiation therapy (CyberKnife system, Accuracy Incorporated). Nine patients who had been pretreated with leuprolide (Lupron, Abbott) endocrine deprivation and three patients with recurrent prostate cancer were excluded from the study because previous treatment might have altered the biologic properties of the tumor and response to subsequent robotic stereotactic body radiation therapy. The other 87 patients formed the study group. Seventy-three of the 87 patients underwent robotic stereotactic body radiation therapy monotherapy to a dose of 38 Gy delivered in four fractions. Fourteen patients underwent robotic stereotactic body radiation therapy as a boost to 21 Gy delivered in two fractions in combination with whole-pelvis intensity-modulated radiation therapy (IMRT) to a dose of 41.4 Gy delivered in 23 fractions. Patients with a favorable prognosis (digital rectal examination category T1–T2b, Gleason score ≤ 6, PSA concentration ≤ 10 ng/mL) and selected patients with an intermediate prognosis (Gleason Score 7 or PSA concentration 10.1–20 ng/mL if other favorable characteristics were present) underwent robotic stereotactic body radiation monotherapy. This therapy as a boost in conjunction with whole-pelvis IMRT was administered to patients with more advanced disease, who presented more adverse prognostic features yet had no evidence of disease beyond the periprostatic region. In the

patients with advanced disease, the whole-pelvis IMRT component was added to cover the higher probability of subclinical disease beyond the confines of the prostate.

Retrospective review of the MR images and clinical information was approved by the investigational review board at our institution, who waived the requirement for written informed consent. Robotic stereotactic body radiation monotherapy was performed under a clinical trial, which was approved by the investigational review board with written informed consent. The patients had been referred for clinical pretreatment and posttreatment MRI.

Patients

All 87 men who formed the study group (mean age, 68.5 years; range, 53–81 years) had biopsy-proven prostate cancer. Table 1 shows patient data for the 73 patients who underwent robotic stereotactic body radiation monotherapy and the 14 patients who underwent combined robotic stereotactic body radiation therapy and IMRT.

MRI

All patients underwent imaging with a 1.5-T MRI system (Signa HDx, GE Healthcare) equipped with echo-speed gradients (33 mT/m, 120 mT/m/s), HDx system software (GE Healthcare), and an external phased-array surface coil. MRI included T1-weighted, T2-weighted, and dynamic gadolinium-enhanced perfusion sequences. Table 2 shows the imaging parameters for each sequence. All 87 patients underwent pretreatment MRI. MRI was repeated serially after radiation therapy at 2 months for 22 patients, 6 months for 71 patients, 12 months for 54 patients, and 24 months for 27 patients.

Dynamic Gadolinium-Enhanced MRI

DCE-MRI was performed in the axial plane with 16 sections through the prostate with a 22-cm FOV. Images in three unenhanced phases were obtained before injection of 0.1 mmol/kg gadobenate dimeglumine (MultiHance, Bracco Diagnostics) to be averaged as baseline. The contrast injection rate was adjusted for a total injection time of 10 seconds. After a 20-second scan delay, multiphase 3D fast spoiled gradient-echo acquisition was continued. A total of 20 contrast-enhanced phases with

a temporal resolution of 19 s/phase was obtained for 6 minutes 20 seconds. The scanning parameters for the dynamic 3D fast spoiled gradient-echo sequence are shown in Table 2.

Processing the Dynamic Contrast-Enhanced MR Images

Interpretation and postprocessing of the DCE-MRI dataset was performed at a computer-aided detection (CAD) workstation (CADvue, iCAD). The 368 images from the 20 dynamic phases of DCE-MRI were sent directly from the MRI unit to the CAD server. The DCE-MRI dataset was automatically processed with the CAD perfusion analysis software, which generated colorized parametric maps, subtraction images, and quantitative values for each region of interest drawn. The pharmacokinetic analysis was performed with the Tofts two-compartment model [18, 19]. The model has wide application and has been used for prostate perfusion analysis [21–24]. For enhancing voxels, the transfer constant K^{trans} (permeability surface area product per unit volume of tissue, reported in $minutes^{-1}$) and the rate constant k_{ep} (efflux rate from extravascular extracellular space back to plasma, also reported in $minutes^{-1}$) were calculated to fit the gadolinium concentration curves to the model. The extravascular extracellular space volume fraction per unit volume of tissue (v_e) was calculated as K^{trans}/k_{ep} . Those parameters were displayed as colorized maps overlaid on gray-scale DCE-MRI baseline images, and the actual values were extracted by use of the various charts available through the CAD workstation.

Robotic Stereotactic Body Radiation Therapy

The inclusion criteria for robotic stereotactic body radiation therapy were biopsy-proven prostate cancer with no evidence of extracapsular tumor spread, involvement of the seminal vesicles, and presence of regional nodal or distant metastasis. The planning target volume in all cases included the prostate as defined by our prostate MRI protocol 3D coregistered with prostate CT scans matching fiducial to fiducial plus up to 2 cm of contiguous seminal vesicle and a 2-mm volume expansion in all directions, except posterior, where the prostate abutted the rectum. In that location, the margin expansion was reduced to zero, justified by robotic stereotactic body radiation therapy system

MRI of Prostate Cancer

TABLE 2: Parameters for Complete MRI Examinations of the Prostate

Pulse Sequence	TR	TE	Matrix Size	No. of Signals Acquired	Slice Thickness (mm)	Gap (mm)	FOV (cm ²)	Flip Angle	Plane	Note	Time (min)
T1-weighted SGE	145	4.4	256 × 256	5	5	0.5	22	80°	Axial		6:14
T2-weighted fast-recovery FSE	3517	85	256 × 256	3	3	0.3	22	90°	Axial		5:52
T2-weighted fast-recovery FSE	2350	85	256 × 256	3	3	0.3	22	90°	Coronal		2:30
T2-weighted fast-recovery FSE	2067	85	256 × 256	2	3	0.3	22	90°	Sagittal		2:30
3D FSPGR DCE	3.21	1.49	160 × 160	2	4	0	22	12°	Axial	16 slices × 20 phases	6:20
3D FSPGR Dixon ^a	7.06	2.39	320 × 288	1	4.4	-2.2	40	12°	Axial/coronal	Dixon water	0:26
2D SGE	150	1.95	320 × 320	2	3	0.3	24	70°	Axial	Fat saturated	4:52

Note—SGE = spoiled gradient-echo, FSE = fast spin-echo, FSPGR = fast spoiled gradient-echo, DCE = dynamic contrast-enhanced.

^a3D FSPGR with Dixon water reconstruction (LAVA-Flex, GE Healthcare). LAVA = liver acceleration volume acquisition.

targeting accuracy [21–25] and reports that prostate cancer does not invade posteriorly in the midline beyond the Denonvilliers fascia.

Patients at intermediate risk had a 5-mm dorsolateral prostate-to-planning target volume expansion to account for the increased risk and the potential distance of extracapsular extension near the neurovascular bundle [9–11]. Typically, the 2-mm margin expansion used in patients who have a favorable prognosis split the neurovascular bundle as defined on MR images, theoretically producing an element of nerve sparing to at least the outer aspect of the neurovascular bundle. The 5-mm expansion used for patients with an intermediate prognosis fully encompassed it.

In addition to the DCE-MRI series, we also used standard T1-weighted gadolinium-enhanced and T2-weighted MRI sequences. We imported both image types into the robotic stereotactic body radiation therapy treatment planning computer to facilitate capsular definition of the prostate, apical definition, tumor visualization, visualization of the neurovascular bundle, and visualization of implanted gold fiducial markers to enable the most comprehensive combination of prostate anatomic evaluation and accurate MR-to-CT image coregistration. The urethra was identified by insertion of a Foley catheter, which also was a reference structure for MR-to-CT image coregistration.

Clinical Follow-Up

After robotic stereotactic body radiation therapy, the patients underwent routine regular follow-up clinical examinations. Serial measurements of serum PSA concentration were obtained 2, 6, 12, 18, and 24 months after treatment.

Review of MR Images

The DCE-MR images of the prostate were evaluated at a workstation (CADvue, iCAD) by one radiologist with 20 years of experience interpreting

body MR images. The reviewer was blinded to results of prostate biopsy and clinical data, including serum PSA concentration. Results were recorded prospectively at the time of initial study interpretation. The DCE-MRI parametric maps and conventional MR images were reviewed concurrently. The size and location of any focally enhancing tumors in the peripheral zone were recorded.

On the tricolor parametric maps, enhancing tumors of the peripheral zone with rapid contrast uptake and rapid washout with k_{ep} values greater than 6 minutes⁻¹ (red) or rapid uptake and plateau kinetics with intermediate k_{ep} values (3–6 minutes⁻¹) (green) were recorded as tumors. Any areas of suspicious enhancement in the transitional zone or central zone were discounted because it is known that DCE-MRI alone is not specific in those areas [25], and benign prostatic hypertrophy has dynamic patterns similar to those of cancer. The largest tumor was manually selected by the radiologist as an index lesion to be followed up after robotic stereotactic body radiation therapy by use of serial regions of interest to include the entire tumor or the one-click automated tumor selection feature. For the selected region of interest, the quantitative permeability surface area product (K^{trans}) was extracted for the largest tumor with the CAD software. The height, width, and length of the prostate were recorded, and the prostate volume was calculated as height × width × length × 0.52.

At serial follow-up MRI examinations, the process of MR image review was repeated with measurements of prostate size and volume and assessment of residual tumor on DCE-MR images. The presence of residual tumors on DCE-MRI colorized parametric maps was recorded. Focal nonenhancing areas of necrosis were also noted on the DCE-MR images. The colorized parametric maps were categorized as showing partial response if residual colorized red or green tumor was present in the peripheral zone and complete response if the paramet-

ric maps showed complete resolution of tumor with blue colorization of the peripheral zone. Quantitative analysis was repeated over the area of the initial pretreatment tumor. For each patient, we also calculated the percentage decrease from the baseline pretreatment K^{trans} and prostate volume at follow-up MRI examinations. For the entire study group, the median K^{trans} , prostate volume, and percentage decrease in these values from baseline were calculated for the 2-, 6-, 12-, and 24-month time points.

Correlation With Prostate Biopsy

The ultrasound-guided sextant biopsy reports were reviewed by a single radiologist, and the findings were compared with the DCE-MRI findings. On the basis of the written reports, the sextants involved with tumor were tabulated for the prostate biopsy and recorded for the right base, right midportion, right apex, left base, left midportion, and left apex. The dominant mass was recorded according to the number of biopsy cores with positive results and the percentage of biopsy specimen involved with tumor. In cases in which sextant biopsy showed similar results for two sextants, the dominant mass was selected in conference with the radiation oncologist. Whether more than one sextant was involved by the dominant mass was recorded. The results of DCE-MRI were similarly tabulated, indicating the prostate sextants involved with tumor on the colorized parametric maps. The dominant mass on the DCE-MR images was recorded, and the sextant or sextants involved were indicated.

We identified in each case whether the imaging and per-sextant biopsy results agreed. In cases in which there was not complete agreement, we categorized whether the biopsy results showed sextants with tumor not identified on the parametric maps and whether the parametric maps showed suspicious areas that were normal according to the biopsy results.

Statistical Analysis

The Wilcoxon matched pairs signed rank test was used to compare pretreatment tumor detection on DCE-MRI parametric maps and pretreatment K^{trans} , serum PSA concentration, and prostate volume with the results 6, 12, and 24 months after radiation therapy. Two-tailed p values are reported. The null hypothesis was rejected at $p < 0.05$.

Results

Dynamic Contrast-Enhanced MRI: Colorized Parametric Maps

Eighty-two patients (94%) had perfusion MRI findings of at least one focal enhancing tumor in the prostate that correlated with a positive biopsy result in the same sextant (Fig. 1). In five patients (four patients with Gleason 6 tumors, one patient with a Gleason 7 tumor) focal lesions were not identified on the perfusion images. In the 82 patients in whom tumors were visualized on the pretreatment DCE-MRI colorized parametric maps, we observed partial resolution of enhancing tumors 2 months after treatment in 15 of 20 patients (75%) and a complete resolution of tumors in 5 of 20 patients (25%). At 6 months, we noted partial resolution of enhancing tumors in 21 of 68 patients (31%) and complete tumor resolution in 47 (69%). At 12 months, we observed partial resolution of enhancing tumors in seven of 51 patients (14%) and complete resolution in 44 (86%). At 24 months, all 25 patients had complete resolution of enhancing tumors. Focal non-enhancing avascular areas in the prostate that might have represented areas of necrosis were observed in 34 of the 87 patients (39%). This finding was initially observed at 6 months in four patients, 12 months in 18 patients, and 24 months in 12 patients.

Quantitative Analysis of Tumor Permeability

For the 82 patients with focal lesions, the median K^{trans} of the tumor on perfusion MR images before robotic stereotactic body radiation therapy was 1.79 minutes⁻¹. Follow-up MRI showed resolution of tumors on the perfusion images with a decrease in size and degree of enhancement. The median tumor K^{trans} decreased to 1.21 minutes⁻¹ at 2 months, 0.39 minutes⁻¹ at 6 months, 0.30 minutes⁻¹ at 12 months, and 0.22 minutes⁻¹ at 24 months. Overall, we observed a 40% decrease in average tumor K^{trans} at 2 months, 75% decrease at 6 months, 82% decrease at 12 months (Fig. 1), and 87% decrease at 24 months. The difference in K^{trans} differed significantly between the pretreatment period and 6 months after

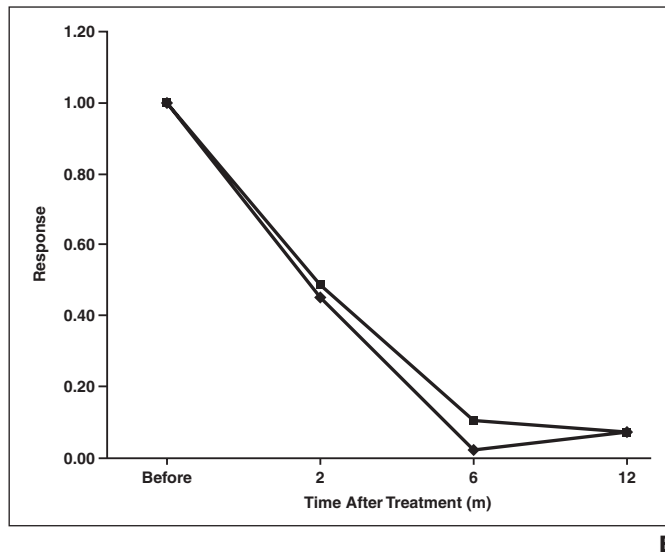
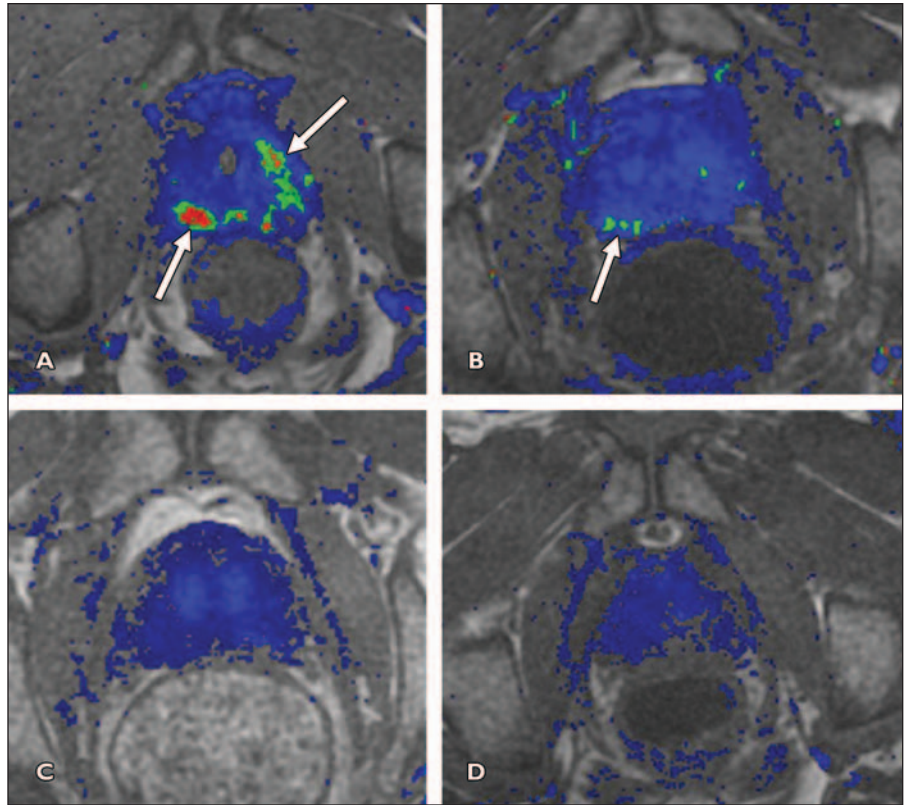


Fig. 1—64-year-old man with Gleason 6 bilateral prostate cancer confirmed with biopsy. **A–D**, Pretreatment dynamic contrast-enhanced MRI (DCE-MRI) colorized permeability map (**A**) depicts bilateral peripheral zone tumors (arrows) (median K^{trans} , 1.79 minutes⁻¹; prostate-specific antigen [PSA] concentration, 8.2 ng/mL). Follow-up DCE-MR image 2 months after radiation therapy (**B**) shows interval improvement with decreasing tumor (arrow) (median K^{trans} , 0.87 minutes⁻¹; PSA concentration, 3.7 ng/mL). DCE-MR image 6 months after radiation therapy (**C**) shows resolution of all enhancing tumors (median K^{trans} , 0.19 minutes⁻¹; PSA concentration, 1.8 ng/mL). DCE-MR image 12 months after radiation therapy (**D**) shows decreased enhancement of prostate with no evidence of residual or recurrent tumor (median K^{trans} , 0.13 minutes⁻¹; PSA concentration, 0.6 ng/mL). **E**, Graph of standardized serial PSA concentration (◆) and DCE-MRI tumor permeability surface area product (K^{trans}) (■) before and after radiation therapy shows percentage decrease compared with pretreatment values. Progressive decline in serum PSA concentration and K^{trans} indicates response of prostate cancer to radiation therapy.

MRI of Prostate Cancer

TABLE 3: Prostate Cancer K^{trans} Values Compared With Gleason Score

Time (mo)	Gleason Score					
	6		7		8 or 9	
	K^{trans} (min ⁻¹)	<i>n</i>	K^{trans} (min ⁻¹)	<i>n</i>	K^{trans} (min ⁻¹)	<i>n</i>
Pretreatment	1.21	43	1.65	33	2.26	11
2	0.34	12	1.62	6	1.65	4
6	0.22	37	0.29	24	0.26	10
12	0.18	28	0.21	19	0.17	7
24	0.13	15	0.21	9	0.14	3

Note— K^{trans} is the median tumor value obtained from dynamic contrast-enhanced MR images of patients with prostate cancer. Gleason score is determined from pathologic evaluation of prostate biopsy specimen. *n* = number of patients. One patient with a Gleason score of 5 was included in the Gleason 6 category.

treatment and between 6 and 12 months after treatment ($p < 0.05$). The K^{trans} values at 12 and 24 months did not differ significantly ($p > 0.05$).

Calculation of tumor K^{trans} was related to prostate cancer Gleason score (Table 3 and Fig. 2). Gleason 6 tumors had a median K^{trans} of 1.21 minutes⁻¹ before robotic stereotactic body radiation therapy; Gleason 7 tumors, 1.65 minutes⁻¹; and Gleason 8 or 9 tumors, 2.26 minutes⁻¹ ($p < 0.05$). These differences in tumor K^{trans} persisted 2 months after treatment, at which time Gleason 6 tumors had a median K^{trans} of 0.34 minutes⁻¹; Gleason 7 tumors, 1.62 minutes⁻¹; and Gleason 8 or 9 tumors, 1.65 minutes⁻¹ ($p < 0.05$). Six and 12 months after treatment, there was no significant difference in tumor K^{trans} values for the different Gleason score categories.

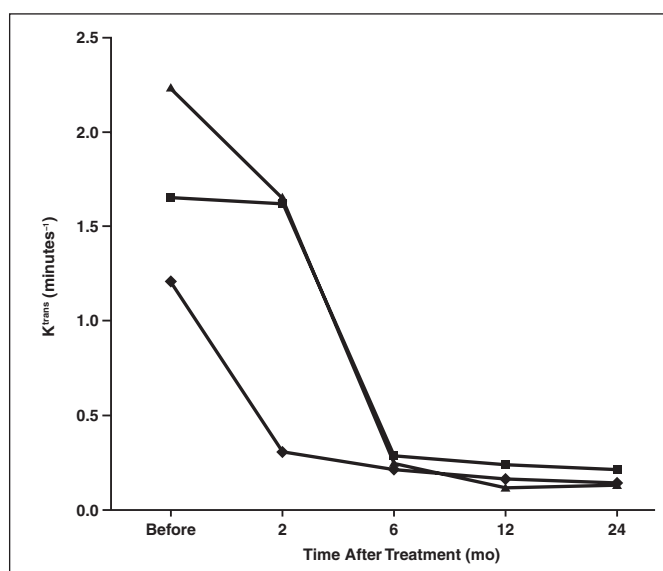
Prostate Volume

The volume of the prostate decreased after robotic stereotactic body radiation therapy (Table 4). Compared with baseline prostate volume, a 23% decrease was found at 2 months, 26% decrease at 6 months, 33% decrease at 12 months, and 37% decrease at 24 months ($p < 0.05$).

Serum Prostate-Specific Antigen Concentration

The median PSA concentration before robotic stereotactic body radiation therapy was 6.45 ng/mL. Two months after treatment, the concentration was 2.90 ng/mL; 6 months, 1.30 ng/mL; 12 months, 1.10 ng/mL; and 24 months, 0.59 ng/mL ($p < 0.05$). Two months after treatment, we observed an interval decrease in serum PSA concentration of 58%; 6 months, 77%; 12 months, 82%; and 24 months, 88%. PSA relapses occurred in two patients with increasing serum PSA concentrations: one patient 12 months and one patient 24 months after treatment. Both patients had been treated with combined ro-

Fig. 2—Graph shows relation between Gleason score (◆, 6; ■, 7; ▲, 8 or 9) before and serial measurements of prostate cancer median K^{trans} obtained from dynamic contrast-enhanced MR images obtained from pathologic evaluation of endorectal biopsy specimens before and after treatment.



botic stereotactic body radiation therapy and IMRT. Both of these patients had evidence of distant tumor recurrence. Follow-up DCE-MRI of both patients showed no evidence of residual or recurrent tumor.

Seven patients experienced PSA bounce—the phenomenon in which PSA concentration increases temporarily after radiation therapy—1 year after robotic stereotactic body ra-

diation therapy (Fig. 3). The corresponding DCE-MRI showed no residual tumor in six patients. Follow-up serum declining PSA concentrations in all six patients did confirm absence of tumor. In one patient with PSA bounce 12 months after treatment, DCE-MRI showed increased colorization. This patient had clinical evidence of prostatitis. Follow-up examinations showed a slowly de-

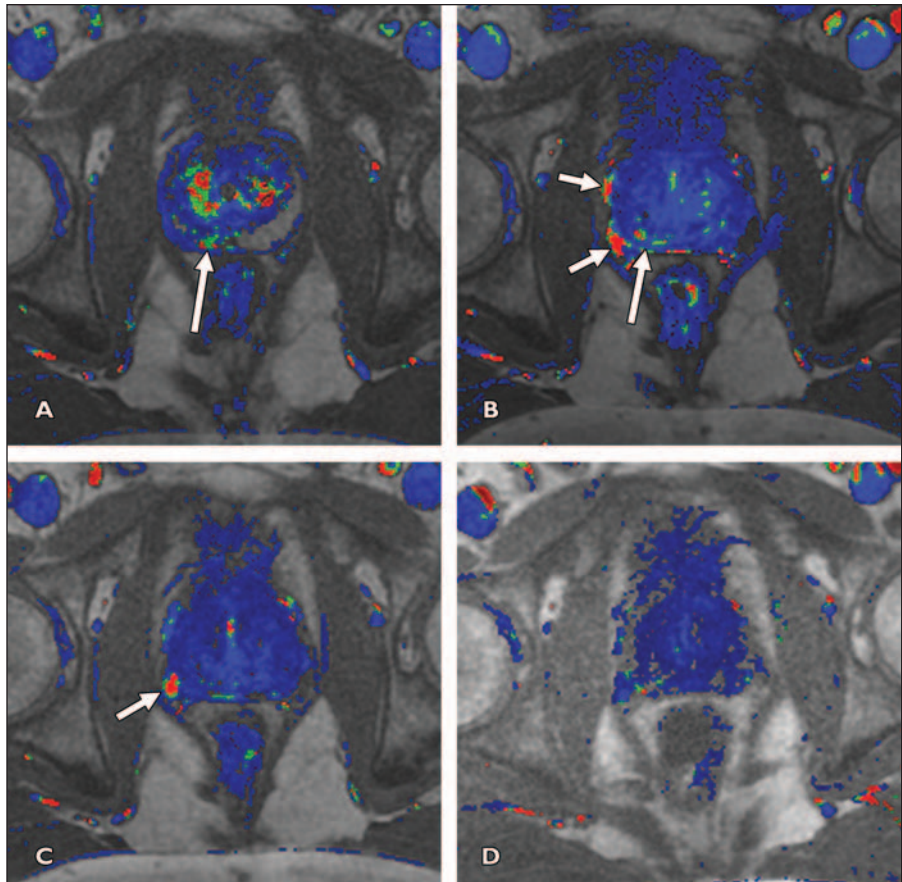
TABLE 4: Measurement of Response of Prostate Cancer to Robotic Stereotactic Body Radiation Therapy

Time (mo)	Prostate-Specific Antigen Concentration (ng/mL)	Volume (cm ³)	K^{trans} (min ⁻¹)
Pretreatment	6.45	41.2	1.79
2	2.90	35.3	1.21
6	1.30	30.3	0.39
12	1.10	29.0	0.30
24	0.59	26.6	0.22

Note—Values are median prostate-specific antigen concentration, prostate volume, and K^{trans} from dynamic contrast-enhanced MR images of 87 patients with prostate cancer. Measurements were obtained before treatment and 2, 6, 12, and 24 months after treatment.

Fig. 3—55-year-old man with Gleason 6 prostate cancer and prostate-specific antigen (PSA) bounce 12 months after robotic stereotactic body radiation therapy.

A–D, Pretreatment colorized parametric map (**A**) shows focal right posterior peripheral zone tumor (*arrow*) that correlated with biopsy results (K^{trans} , 0.81 minutes⁻¹, serum PSA concentration, 5.1 ng/mL). Colorized parametric map obtained 6 months after treatment (**B**) shows partial resolution of right posterior prostate tumor (*long arrow*); periprostatic vessels (*short arrows*) are evident (K^{trans} , 0.45 minutes⁻¹, serum PSA concentration, 1.3 ng/mL). Colorized parametric map 12 months after treatment (**C**) shows near-complete resolution of right-sided tumor although serum PSA concentration has increased (K^{trans} , 0.28 minutes⁻¹, serum PSA concentration, 2.5 ng/mL). Periprostatic vessel (*arrow*) is evident. Colorized parametric map 24 months after treatment (**D**) shows no residual tumor; serum PSA concentration has declined (K^{trans} , 0.19 minutes⁻¹, serum PSA concentration, 1.7 ng/mL). **E**, Graph of standardized serial PSA values (◆) and dynamic contrast-enhanced MRI tumor permeability surface area product (K^{trans}) (■) before and after robotic stereotactic body radiation therapy shows increase in serum PSA concentration 12 months after treatment. PSA concentration subsequently declined without additional treatment. This false-positive PSA bounce occurs after radiation treatment. Steady decline in serial K^{trans} values from DCE-MRI indicates response of tumor to robotic stereotactic body radiation therapy.



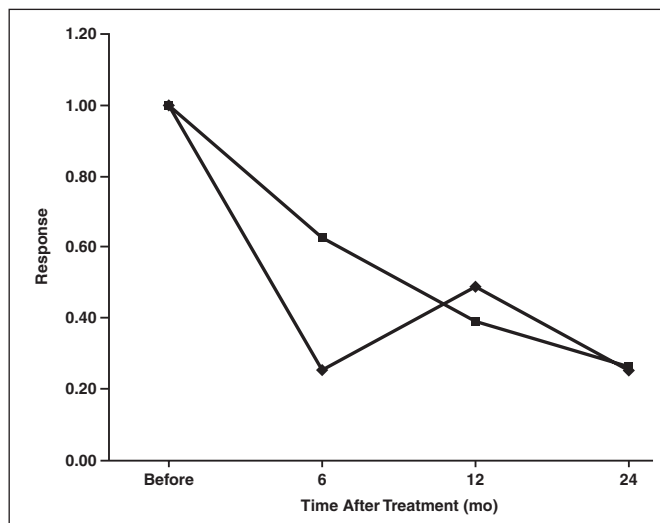
clinical serum PSA concentration and resolving DCE-MRI findings.

In nine patients, the PSA response was slow with either a plateau of the elevated PSA concentration 1–2 years after treatment or a 2-year serum PSA concentration more than 1 SD above the median value for all patients. In this group, corresponding DCE-MRI showed no residual tumor in eight patients. Follow-up serum PSA concentration subsequently declined in all eight patients, indicating continuing tumor response. In one patient, DCE-MRI showed new small areas of colorization in the peripheral zone. Clinical follow-up showed further decline in serum PSA concentration, suggesting false-positive findings on the DCE-MRI color parametric maps.

Correlation With Prostate Biopsy

In 70 patients (80%) the dominant tumor finding at biopsy agreed with the dominant enhancing tumor depicted on the DCE-MRI colorized parametric maps (Fig. 4). The sextants involved with tumor at prostate biopsy agreed with the DCE-MRI findings in all six sextants in 55 of the 87 patients (63%), in five of six sextants in 23 patients, in four of six sextants in four, in three of six sextants in two patients, and in two of six sextants in one patient.

In 32 cases (37%) there was disagreement regarding the sextants involved with tumor.



E

In 10 patients (11%) prostate biopsy showed sextants involved with tumor not confirmed with DCE-MRI. This group included the five patients whose DCE-MRI colorized parametric maps showed no tumor. In 22 cases (25%) the DCE-MRI colorized parametric maps showed additional sextants suspicious for tumor that were normal at biopsy. In 20

cases (23%) the DCE-MRI findings suggested the presence of suspicious contralateral regions not found at prostate biopsy.

Discussion

The role of DCE-MRI in evaluation before radiation therapy and for monitoring the response of prostate cancer to robotic stereotactic

MRI of Prostate Cancer

body radiation therapy has not been evaluated, to our knowledge. Our study showed that DCE-MRI was a robust means of depicting tumors before treatment; 94% of patients had tumors with increased vascular permeability. After treatment, we observed a consistent resolution of prostate cancer on the DCE-MR images. Qualitatively, the tumors typically resolved on the colorized parametric maps within 6 months after radiation therapy. Quantitatively, we observed a 75% decrease in K^{trans} of the tumors within 6 months and a continued slight decrease 12–24 months after treatment.

In previous studies in which Toft two-compartment model analysis was used, the results were compared with those of histopathologic evaluation with either whole-mount preparation of the excised prostate or step-section sextant analysis of the prostate [26, 27]. Addition of the DCE-MRI images improved staging accuracy and tumor detection [27] and assessment of extracapsular tumor spread [26]. The role of DCE-MRI in evaluating response of prostate cancer to IMRT has been reported [28]. In a study of six patients who underwent DCE-MRI before and 3 and 12 months after IMRT, the investigators found a significant decrease in perfusion and vascular volume of prostate tumors after therapy.

Pending long-term confirmation of the promising intermediate-term results, robotic stereotactic body radiation therapy appears to be an attractive therapeutic option for monotherapy for early-stage prostate cancer. The treatment is efficient and noninvasive and effectively addresses the shortcomings of other treatments of early-stage prostate cancer [9–11]. Five-year results of robotic stereotactic body radiation therapy for prostate cancer have shown a biochemical progression-free survival rate of 93% [11]. Robotic stereotactic body radiation therapy also is a useful boost technique in advanced cases, in combination with external beam radiation therapy. The dosimetry coverage is comparable to that of high-dose-rate brachytherapy boosting but without the indwelling plastic tubes.

After radiation therapy, serum PSA concentration continues to be the best biologic indicator of active tumor. PSA measurement, however, is limited by false-positive and false-negative results and by inability to localize primary or recurrent tumors within the gland [3–7]. Serum PSA concentration does not always decrease in a consistent manner, even if the patient has been successfully treated, and PSA bounce, characterized by a temporary posttreatment increase in PSA concentration, is common with all

forms of radiation therapy, including robotic stereotactic body radiation therapy [6, 7]. The reported incidence of PSA bounce after brachytherapy for prostate cancer was 32% in a study in which 295 patients underwent follow-up for 3 years [7]. Parallel review of DCE-MRI yields additional data to help assess whether a suboptimal PSA response or PSA bounce reflects local failure of treatment or a false-positive PSA result, thereby guiding more accurate clinical decision making when PSA interpretation is difficult.

After external beam radiation therapy for prostate cancer, the reported 5-year PSA relapse rate ranges from 15% for patients at low risk to 67% for patients at high risk [1, 2]. Evaluation of patients with biochemical failure after radiation therapy is challenging [2]. Biopsy after radiation therapy can have false-negative results due to sampling error and false-positive results due to slow tumor regression. Biopsy findings can be indeterminate, showing radiation changes combined with residual tumor of uncertain viability [2]. In this complex clinical setting, MRI and MR spectroscopy may play a role in evaluation for local tumor recurrence [29]. DCE-MRI of the prostate can be used to detect tumor recurrence after therapy and for localization of prostate cancer before repeat biopsy [30]. Haider et al. [23] found that DCE-MRI performs better than T2-weighted MRI in the detection and localization of prostate cancer in the peripheral zone after external beam radiation therapy. Sextant sensitivity was 72% for DCE-MRI and 38% for T2-weighted MRI.

DCE-MRI quantitative analysis also provides intriguing possibilities for correlating tumor aggressiveness with the parametric values used to assess tumor vascularity.

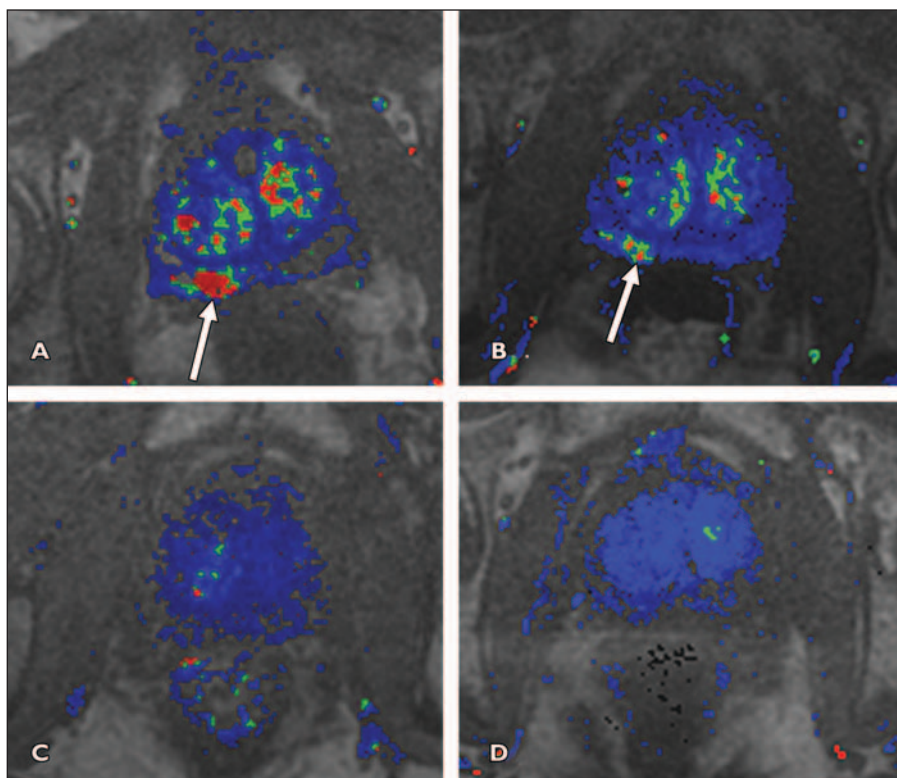


Fig. 4—78-year-old man with biopsy-proven Gleason 9 right-sided prostate cancer and 24-month clinical and MRI follow-up results.

A–D, Pretreatment colorized parametric map generated with dynamic contrast-enhanced MRI (DCE-MRI) (**A**) depicts rapidly enhancing tumor (arrow) in right posterior peripheral zone (median K^{trans} , 2.69 minutes⁻¹; prostate-specific antigen concentration, 12.3 ng/mL) and enhancing benign prostatic hypertrophy. Colorized parametric map 6 months after treatment (**B**) shows median K^{trans} of tumor (arrow) has decreased to 2.05 minutes⁻¹ (PSA concentration, 4 ng/mL). Map obtained 12 months after treatment (**C**) shows tumor is no longer visible (K^{trans} , 0.12 minutes⁻¹; PSA concentration, 2.7 ng/mL). DCE-MRI parametric map 24 months after therapy (**D**) shows no residual tumor (K^{trans} , 0.10 minutes⁻¹; PSA concentration, 0.7 ng/mL).

We found that tumors with higher Gleason scores had significantly greater pretreatment K^{trans} values, reflecting higher tumor permeability. These observations are supported by those of previous studies. Schlemmer et al. [31] found that DCE-MRI parametric values can be used to predict microvessel density in prostate cancer and to differentiate low-grade from high-grade tumors. Franiel et al. [32] found that low-grade tumors with a Gleason score less than 6 had a lower mean permeability than high-grade tumors with a Gleason score of 7 or more, higher blood volume, and longer mean transit time.

The limitations of this study included incomplete pathologic proof of tumor location before therapy and of tumor response to robotic stereotactic body radiation therapy. Using biopsy as a standard of reference is an inherent limitation of studies in which nonsurgical treatment is performed. We found incomplete agreement between the results of DCE-MRI and those of sextant prostate biopsy. Enhancing foci on the pretreatment DCE-MR images that were not confirmed at sextant biopsy likely represent undersampling of the prostate at sextant biopsy, although false-positive MRI findings can occur. It is known that incomplete sampling of the prostate at sextant localization can lead to underdiagnosis of cancer [33]. Similarly, identifying the dominant intraprostatic tumor at sextant biopsy as determined by the number of positive cores and percentage of tumor involvement of the core was not always straightforward. Within these limitations, all index lesions on DCE-MR images were chosen to correspond to a site of biopsy-proven prostate cancer at sextant biopsy.

Pretreatment MRI depicted only tumors in the peripheral zone. The 25% of prostate tumors that occur in the transitional zone present challenges in DCE-MRI because angiogenesis also characterizes benign prostatic hypertrophy. Reports have described improved accuracy for central gland tumor detection with T2-weighted and diffusion-weighted MRI [34, 35]. Because the entire prostate was treated with robotic stereotactic body radiation therapy, this limitation did not result in suboptimal treatment.

Improved signal-to-noise ratio can be achieved by imaging with a 3-T MRI system or an endorectal coil. Our decision not to use an endorectal coil was based on the requirements of the radiation oncologist's treatment planning protocol, which demanded precise 3D coregistration of the MRI datasets with CT scans of the prostate. The use of an en-

dorectal coil deforms the prostate so that fusion of the MR images with treatment-planning CT scans would be problematic. The roles of T2-weighted MRI, diffusion-weighted imaging, and spectroscopy for assessing response to robotic stereotactic body radiation therapy were not evaluated in this study.

Technically, our moderate temporal resolution of 19 s/phase can be improved at the expense of less anatomic coverage or spatial resolution or a lower signal-to-noise ratio. Brasch et al. [20] suggested 12 seconds or faster dynamic imaging. Our experience confirms that the tradeoff between temporal resolution and signal-to-noise ratio determines the optimal imaging protocol for DCE-MRI. For other MRI unit and coil combinations, the optimal imaging parameters would have to be determined individually.

Conclusion

Perfusion DCE-MRI has promise for monitoring response of prostate cancer to robotic stereotactic body radiation therapy. After this treatment, DCE-MRI shows decreased perfusion of prostate tumors, indicated by a decline in tumor K^{trans} . In conjunction with serial serum PSA measurement, DCE-MRI can yield additional qualitative and quantitative information about tumor response to therapy, which may be particularly useful in the care of patients with PSA bounce or a slowly responding serum PSA concentration.

References

1. D'Amico AV, Crook J, Beard CJ, DeWeese TL, Hurwitz M, Kaplan I. Radiation therapy for prostate cancer. In: Walsh PC, Retik AB, eds. *Campbell's urology*, 8th ed. Philadelphia, PA: Saunders, 2002:3147–3170
2. Crook J, Malone S, Perry G, Bahadur Y, Robertson S, Abdolell M. Postradiotherapy prostate biopsies: what do they really mean? Results for 498 patients. *Radiat Oncol* 2000; 48:355–367
3. Giri VN, Beebe-Dimmer J, Buyyounouski M, et al. Prostate cancer risk assessment program: a 10-year update of cancer detection. *J Urol* 2007; 178: 1920–1924
4. Nadler RB, Humphrey PA, Smith DS, Catalona WJ, Ratliff TL. Effect of inflammation and benign prostatic hyperplasia on elevated serum prostate specific antigen levels. *J Urol* 1995; 154:407–413
5. Roach M 3rd, Hanks G, Thames H Jr, et al. Defining biochemical failure following radiotherapy with or without hormonal therapy in men with clinically localized prostate cancer: recommendations of the RTOG-ASTRO Phoenix consensus conference. *Radiat Oncol* 2006; 65:965–974

6. Smathers S, Wallner K, Sprouse J, True L. Temporary PSA rises and repeat prostate biopsies after brachytherapy. *Int J Radiat Oncol Biol Phys* 2001; 50:1207–1211
7. Toledano A, Chauvenic L, Flam T, et al. PSA bounce after permanent implant prostate brachytherapy may mimic a biochemical failure: a study of 295 patients with a minimum 3-year followup. *Brachytherapy* 2006; 5:122–126
8. Chang SD, Main W, Martin DP, Gibbs IC, Heilbrun MP. An analysis of the accuracy of the CyberKnife: a robotic frameless stereotactic radiosurgical system. *Neurosurgery* 2003; 52:140–147
9. Fuller DB, Naitoh J, Lee C, Hardy S, Jin H. Virtual HDRSM CyberKnife treatment for localized prostatic carcinoma: dosimetry comparison with HDR brachytherapy and preliminary clinical observations. *Int J Radiation Biol Phys* 2008; 70: 1588–1597
10. King CR, Brooks JD, Gill H, Pawlicki T, Cotrutz C, Presti JC. Stereotactic body radiotherapy for localized prostate cancer: interim results of a prospective phase II clinical trial. *Int J Radiat Oncol Biol Phys* 2008;73:1043–1048
11. Freeman DE, King CR. Stereotactic body radiotherapy for low-risk prostate cancer: five-year outcomes. *Radiat Oncol* 2011; 6:3
12. Macura KJ. Multiparametric magnetic resonance imaging of the prostate: current status in prostate cancer detection, localization, and staging. *Semin Roentgenol* 2008; 43:303–313
13. Ross R, Harisinghani M. New clinical imaging modalities in prostate cancer. *Hematol Oncol Clin North Am* 2006; 20:811–830
14. Katz S, Rosen MM. Imaging and MR spectroscopy in prostate cancer management. *Radiol Clin North Am* 2006; 44:723–734
15. Hricak H, Choyke PL, Eberhardt SC, Leibell SA, Scardino PT. Imaging prostate cancer: a multidisciplinary perspective. *Radiology* 2007; 243:28–53
16. Beyersdorff D, Taymoorian K, Knösel T, et al. MRI of prostate cancer at 1.5 and 3.0 T: comparison of image quality in tumor detection and staging. *AJR* 2005; 185:1214–1220
17. Langer DL, van der Kwast TH, Evans AJ, et al. Prostate tissue composition and MR measurements: investigating the relationships between ADC, T2, K(trans), v(e), and corresponding histologic features. *Radiology* 2010; 255:485–494
18. Tofts PS, Kermode AG. Measurements of the blood-brain barrier permeability and leakage space using dynamic MR imaging. Part I. Fundamental concepts. *Magn Reson Med* 1991; 17:357–367
19. Tofts PS, Brix G, Buckley DL, et al. Estimating kinetic parameters from dynamic contrast-enhanced T(1)-weighted MRI of a diffusible tracer: standardized quantities and symbols. *J Magn Reson Imaging* 1999; 10:223–232

MRI of Prostate Cancer

20. Brasch RC, Li KC, Husband JE, et al. In vivo monitoring of tumor angiogenesis with MR imaging. *Acad Radiol* 2000; 7:812–823
21. Padhani AR, Gapinski J, Macvicar DA, et al. Dynamic contrast-enhanced MRI of prostate cancer: correlation with morphology and tumour stage, histological grade and PSA. *Clin Radiol* 2000; 55:99–109
22. Cheikh AB, Girouin N, Colombel M, et al. Evaluation of T2-weighted and dynamic contrast-enhanced MRI in localizing prostate cancer before repeat biopsy. *Eur Radiol* 2009; 19:770–778
23. Haider MA, Chung P, Sweet J, et al. Dynamic contrast-enhanced magnetic resonance imaging for localization of recurrent prostate cancer after external beam radiotherapy. *Int J Radiat Oncol Biol Phys* 2008; 70:425–430
24. Ocak I, Bernardo M, Metzger G, et al. Dynamic contrast-enhanced MRI of prostate cancer at 3 T: a study of pharmacokinetic parameters. *AJR* 2007; 189:849; [web]W192–W201
25. Seitz M, Shukla-Dave A, Bjartell A, et al. Functional magnetic resonance imaging in prostate cancer. *Eur Urol* 2009; 55:801–814
26. Bloch BN, Furman-Haran E, Helbich TH, et al. Prostate cancer: accurate determination of extracapsular extension with high spatial-resolution dynamic contrast-enhanced and T2-weighted MR imaging—initial results. *Radiology* 2007; 245:176–185
27. Cornud F, Beuvon F, Thévenin F, et al. Quantitative dynamic MRI and localisation of non-palpable prostate cancer. *Prog Urol* 2009; 19:401–413
28. Franiel T, Lüdemann L, Taupitz M, Böhmer D, Beyersdorff D. MRI before and after external beam intensity-modulated radiotherapy of patients with prostate cancer: the feasibility of monitoring of radiation-induced tissue changes using a dynamic contrast-enhanced inversion-prepared dual-contrast gradient echo sequence. *Radiother Oncol* 2009; 93:241–245
29. Coakley FV, The HS, Qayyum A, et al. Endorectal MR imaging and MR spectroscopic imaging for locally recurrent prostate cancer after external beam radiation therapy: preliminary experience. *Radiology* 2004; 233:441–448
30. Rouvière O, Valette O, Grivolat S, et al. Recurrent prostate cancer after external beam radiotherapy: value of contrast-enhanced dynamic MRI in localizing intraprostatic tumor—correlation with biopsy findings. *Urology* 2004; 63:922–927
31. Schlemmer HP, Merkle J, Grobholz R, et al. Can pre-operative contrast-enhanced dynamic MR imaging for prostate cancer predict microvessel density in prostatectomy specimens. *Eur Radiol* 2004; 14:309–317
32. Franiel T, Lüdemann L, Taupitz M, Rost J, Asbach P, Beyersdorff D. Pharmacokinetic MRI of the prostate: parameters for differentiating low-grade and high grade prostate cancer. *Rofa* 2009; 181:536–542
33. Beyersdorff D, Taupitz M, Winkelmann B, et al. Patients with a history of elevated prostate-specific antigen levels and negative transrectal US-guided quadrant or sextant biopsy results: value of MR imaging. *Radiology* 2002; 224:701–706
34. Akin O, Sala E, Moskowitz CS, et al. Transition zone prostate cancers: features, detection, localization, and staging at endorectal MR imaging. *Radiology* 2006; 239:784–792
35. Oto A, Kayhan A, Jiang Y, et al. Prostate cancer: differentiation of central gland cancer from benign prostatic hyperplasia by using diffusion-weighted and dynamic contrast-enhanced MR imaging. *Radiology* 2010; 257:715–723

FOR YOUR INFORMATION

Malpractice Issues in Radiology, 3rd edition, by Leonard Berlin, is now available! For more information or to purchase a copy, see www.arrs.org.